

# MicroNiobium® Steelmaking Alloy Approach in 1080 Wire Rod

This study evaluates different Nb and Nb-V compositions in AISI 1080 steels for wire rod applications. The process and product metallurgical improvements relate to the Nb-pinning effect of the austenite grain boundaries and the refinement effect in pearlitic eutectoid steel for pre-stressed concrete wire rod. Although the Nb solubility is limited in high-carbon steels compared to low-carbon steels, the optimized Nb content is defined based on experimental results.

## Author



**Steven G. Jansto**

market and technical  
development manager, CBMM  
North America Inc., Bridgeville,  
Pa., USA  
jansto@cbmmna.com

The MicroNiobium® alloy approach is applied in higher-carbon steels exceeding 0.20% carbon. This study evaluates different Nb and Nb-V compositions from 0.020 to 0.120% Nb in AISI 1080 steels for wire rod applications. Although the Nb solubility is limited in high-carbon steels compared to low-carbon steels, the optimized Nb content is defined based on experimental results. The optimized Nb content leads to improved mechanical properties due to the finer interlamellar pearlite spacing. Seven different eutectoid steel developmental chemistries were evaluated to determine the effectiveness of Nb, V or Nb-V concentrations on the pearlite interlamellar spacing, mechanical properties and drawability consistency.

## Background Information

Several niobium (Nb)-containing high-carbon steel applications over the past several years have employed the thermomechanical controlled processing (TMCP) approach in higher-carbon engineering tool steels and high-carbon long product applications. Generally, the TMCP in some lower-carbon engineering steels apply Nb at

concentrations of 0.030–0.045%. However, the application of Nb in higher-carbon steels such as AISI 1080 has been quite limited. Although the Nb solubility is lower compared to low-carbon steels, the grain refinement attribute of Nb still applies. Through empirical evidence and actual operating data, the MicroNiobium alloy approach has demonstrated some very positive results on high-carbon grades such as steel wire rods and bars, eutectoid steels such as rail, and other medium-carbon engineering alloy applications. This technology has been introduced at an accelerated pace throughout the world.

Historically, Nb has not been the microalloy of choice in high-carbon steels because of the predicted lower solubility of the Nb carbonitrides in higher-carbon steels. Although there is lower solubility, current industrial applications validate the effectiveness of Nb in the grain refinement and precipitation strengthening mechanism in Nb-only and Nb-modified V-containing steels. Over the past two decades, within this higher-carbon steel segment, metallurgical research studies did not typically show the positive results of Nb in high-carbon grades. The reason was that researchers incorporated Nb

This article is available online at AIST.org for 30 days following publication.

levels greater than necessary and, consequently, less than favorable mechanical properties were reported and the cost increased for these grades. Again, high-carbon Nb metallurgy is different from low-carbon metallurgy due to the solubility differences and the process metallurgy considerations.

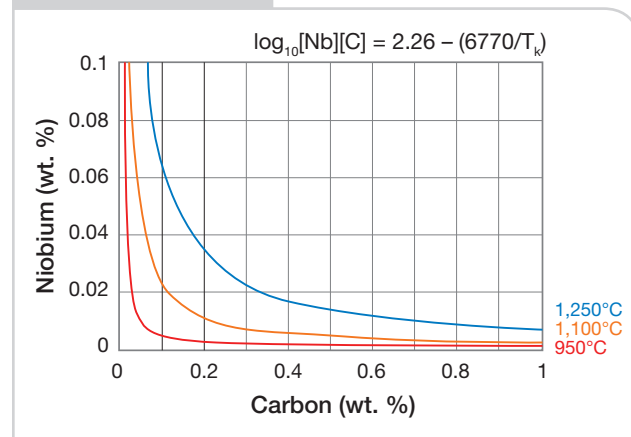
In the past, Nb levels exceeding 0.040% were thought necessary in order to obtain proper grain refinement in high-carbon steels for microstructural control to achieve required mechanical properties. However, high-carbon metallurgical and production experience to date has in fact indicated that the elevated Nb levels in high-carbon steels certainly make processing more challenging, and the resultant properties may not always be optimized. So, there was a reluctance to accept the role of Nb by the high-carbon steel producers and end-user market over the past several decades. This study specifically analyzed a variety of Nb levels ranging from 0.02% to 0.12% Nb, some Nb+V combinations and V levels up to 0.092%, and compared the mechanical property and wire drawing performance. It is important to consider the synergistic precipitation behavior effect between the Nb and V, which may contribute to the improved mechanical performance. Also, duplex V-Nb carbonitride, or in some cases a V-Nb-Mo carbonitride triplex complex, precipitation behavior requires further study.

High-carbon steel process metallurgy (including melting and hot rolling) is infrequently reported from industrial producers. However, this research encompasses both laboratory heats and then validation with industrial heats. Based on operational experience, the optimization of Nb content and the proper control of the reheat furnace are quite critical in the production of such microalloyed high-carbon steel grades. An optimum Nb concentration may be directly correlated to a given carbon level, depending on the reheat furnace process metallurgy parameters, heating practices and combustion at a given mill. For example, reheating high-carbon (>0.50% C) billets and slabs can be enhanced through the incorporation of combustion practices resulting in an air-to-gas ratio less than 1.00.

The reluctance by others to consider the application of Nb in higher-carbon steels (greater than 0.20% C) is depicted by the solubility relationship of Nb versus C content, illustrated in Figure 1.

**Ductility Wire Drawing Considerations** — The most important parameters in the wire drawing operation are the amount of reduction, the die angle  $2\alpha$ , the lubricant and the mechanical properties of the workpiece. The amount of reduction a steel can exhibit, and hence its ductility, are very important measures of the material for any shaping and forming operation, especially for wire drawing. Any incremental

Figure 1



Nb solubility versus C content.

increase in the ductility of wire rods results in the distinct advantage of eliminating heat treatment and obtaining high strength levels. Also, the relationship established by Embury and Fisher has been widely applied in the wire industry for estimation of the strength of cold drawn eutectoid steels.<sup>1</sup> These calculations also indicate that the increase of the drawing strain through the improvement of ductility is one of the most effective ways to increase the strength of cold drawn pearlitic steels:

$$\sigma = \sigma_o + [k/(2\lambda_o)^{1/2}] \cdot \exp(\epsilon/4) \quad (\text{Eq. 1})$$

where

$\epsilon$  = true drawing strain,

$\sigma_o$  = friction stress,

$\lambda_o$  = initial interlamellar spacing and

$k$  = Hall-Petch parameter.

Interlamellar spacing is one of the most suitable factors to control the ductility of pearlitic steels. In eutectoid steels, the refinement of interlamellar spacing causes a reduction in the cementite thickness, regardless of the method applied. Refinement may be achieved through hot rolling thermal practices, special heating practices and/or chemical compositional effects through microalloying. Coarse pearlite deforms inhomogeneously and results in strain localization.<sup>2</sup> Therefore, thick cementite in a coarse pearlitic microstructure would exhibit limited ductility and fractures with no thinning. These cracks, due to a shear-cracking process, subsequently turn into cleavage-type cracks during wire processing. Conversely, fine pearlite with very thin cementite exhibits a more uniform distribution of strain during deformation. Thin cementite layers appear to be more ductile and hence, neck down into fragments, resulting in ductile

fracture.<sup>3</sup> Cementite lamellae aligned along the drawing axis are deformed uniformly and thinned to a fibrous shape.<sup>4</sup>

**New Product Development Considerations** — In developing a new steel product application, such as the MicroNiobium approach in 1080 steel, attention must be paid to important issues such as:

1. The possibility to design a steel grade that will assist in the elimination or simplification of one or more secondary and ternary processing steps, thereby improving productivity and reducing manufacturing costs.
2. The possible improvement of the new product functionality, longer service life, reduced weight or new advantages to the final product.
3. Whether it is possible to eliminate environmentally harmful substances during the processing.

These requirements are not always compatible. Therefore, it is important to proceed with developmental steps based on a good understanding of the operational conditions at the processing stages, the use condition and the characteristics of the final product for which the steel will be applied.

Most recently, development of the MicroNiobium alloy approach with Nb concentrations of 0.005–0.020%Nb has been successfully applied to the following medium- and high-carbon steel grades and applications:

1. AISI 5160 and 9259 automotive coil springs.
2. AISI 1050 automotive fasteners.
3. S500 earthquake/fire-resistant reinforcing bars.
4. 0.20% C abrasion-resistant plates for heavy machinery and agricultural machinery.
5. Eutectoid steels for rail and pre-stressed wire rod.
6. Carburized steel power transmission components such as 4130 and 6250 grades.

## Experimental Procedure

Experimental laboratory heats were produced with Nb, V and Nb+V and then cast in a vacuum furnace. The objective was to compare the mechanical properties and drawability during wire rod production of a single microalloy addition of Nb against a V addition against a dual Nb+V combination. The compositions melted are shown in Table 1.

Laboratory ingots were welded to industrial billets of similar carbon grades and hot rolled at an industrial operation into 11-mm-diameter wire rods following standard reduction and thermal practices for pre-stressed concrete (PSC) wire rod. The wire rods were characterized by optical microscopy, scanning electron microscopic (SEM) examination and tensile tests. The pearlitic interlamellar spacing was measured using the line intercept method with the SEM. The austenite grain size was measured utilizing the NFA 04-102 standard method. The hot rolled wire

Table 1

Chemical Compositions of Experimental Heats (in %)								
	S0	V1	V2	VNB	NB1	NB2	NB3	NB4
C	0.829	0.778	0.776	0.781	0.811	0.770	0.805	0.791
Mn	0.756	0.707	0.731	0.730	0.760	0.635	0.736	0.723
Si	0.221	0.234	0.218	0.205	0.221	0.193	0.228	0.230
Al	0.004	0.003	0.002	0.002	0.005	0.002	0.008	0.005
Cr	0.144	0.138	0.152	0.150	0.152	0.124	0.156	0.157
Nb	0.002	0	0.002	0.021	0.023	0.038	0.087	0.119
V	0.002	0.092	0.053	0.050	0.003	0	0	0
N (ppm)	69	73	67	73	70	70	70	85

Table 2

Chemical Composition of Industrial Heat (in %)						
C	Mn	P	S	Si	Cr	Nb
0.830	0.773	0.011	0.012	0.237	0.270	0.018

Table 3

Surface Defect Incidence on Wire Rods

Length ( $\mu\text{m}$ )	Wire rod samples (point count of surface defects observed; L = length; D = depth)															
	S0		V1		V2		VNB		NB1		NB2		NB3		NB4	
	L	D	L	D	L	D	L	D	L	D	L	D	L	D	L	D
20–50	15	19	9	9	22	23	9	10	10	14	10	12	0	3	0	0
51–100	3	1	1	1	8	7	1	0	0	0	3	2	1	1	1	3
100–150	0	1	0	0	1	1	0	1	1	1	1	0	0	1	1	3
>150	4	1	1	1	3	3	1	0	0	0	0	0	1	1	2	0

rods were then cold drawn in the laboratory. Their mechanical behavior was investigated through tension and torsion tests after each drawing pass.

Table 4

Mechanical Properties Based on Tensile Tests

Wire rod sample	Yield strength 0.2% ( $\text{N/mm}^2$ )	Tensile strength ( $\text{N/mm}^2$ )	Reduction of area (%)
S0	627	1,086	30.4
V1	733	1,154	26.8
V2	719	1,154	22.9
VNB	740	1,169	38.0
NB1	648	1,139	45.1
NB2	680	1,102	41.4
NB3	666	1,115	38.4
NB4	709	1,150	35.8

Subsequent to the evaluation of the laboratory heats, an industrial heat was produced with a 0.018% Nb composition. The chemical composition of the industrial heat is shown in Table 2.

Two sets of samples were taken from two different wire drawing plants after each drawing pass. The drawing pass data were used to establish the work-hardening curves of the steel. The wire rods produced from the industrial heat have a higher Cr content, leading to a higher tensile strength.

## Results

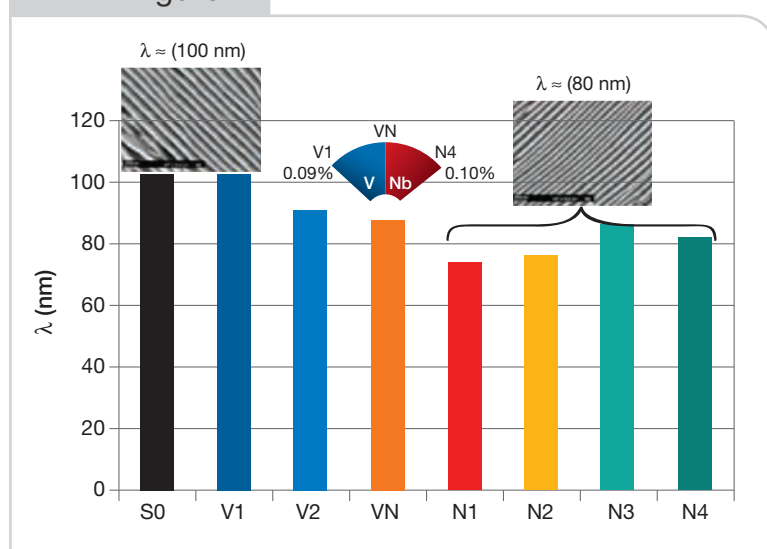
The microstructure of the laboratory-produced wire rods was homogeneous and pearlitic for all of the experimental steels. Optical observation did not reveal any incidence of the Nb addition on segregation, decarburization or microstructure homogeneity. The wire rod surface defect levels were compared for all compositions, as shown in Table 3.

The mechanical properties of the wire rods are shown in Table 4.

Generally, the tensile strength levels are of the same order for the V-containing or Nb-containing steels; however, the Nb steel trend is a slightly lower yield strength. Nevertheless, all compositions exceeded the base steel S0 yield strength minimum of 627  $\text{N/mm}^2$  and the 1,086  $\text{N/mm}^2$  tensile strength. As expected, the combination of Nb+V exhibited the highest yield and tensile strength. The important attribute is the consistently higher % reduction of area (RA) for the Nb-containing grades compared to the V-containing grades.

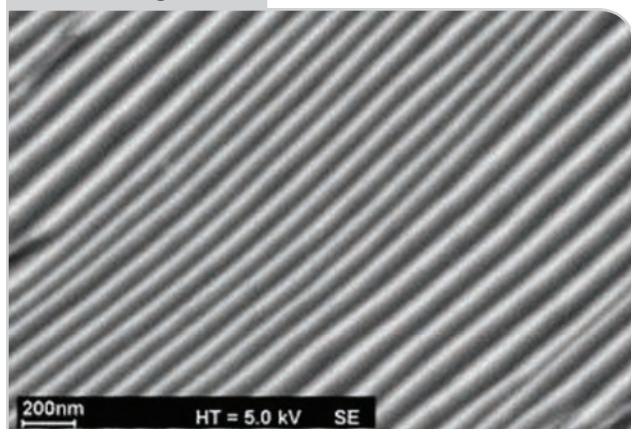
Review of the mechanical property data shows the best elongation with sample NB1, which is the 0.02% Nb MicroNiobium alloy design at 45.1% reduction of area. The yield strength, tensile strength and reduction of area is met, as defined by S0

Figure 2



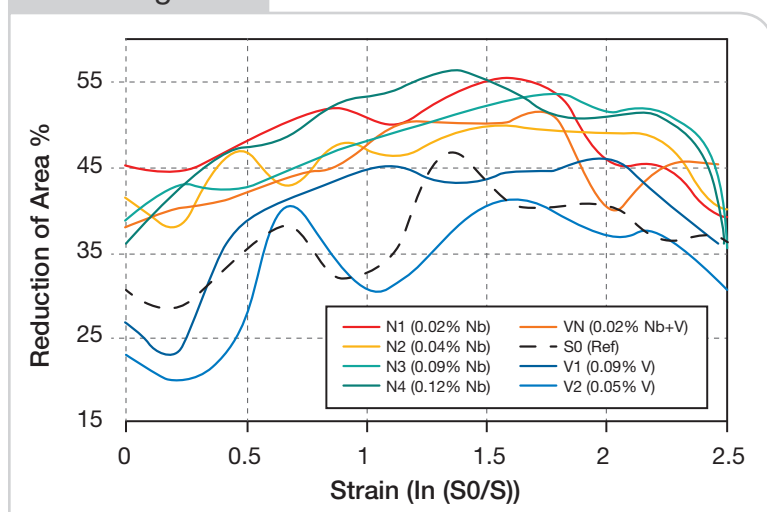
Interlamellar spacing of pearlite in microstructure of as-rolled wire rods.

Figure 3



SEM micrograph of sample NB1 (0.023% Nb) with finest interlamellar spacing.

Figure 4



Reduction of area versus strain.

Table 5

Mean Values of Ultimate Tensile Strength (UTS) and % Reduction of Area (%RA)

UTS (MPa)		%RA	
Coil head	Coil tail	Coil head	Coil tail
1,241	1,253	44.0	43.7

in Table 4. The mechanism of this optimization of the Nb concentration in this high-carbon eutectoid steel is the refinement of the lamellar spacing. As exhibited in Figure 2, the refinement of the lamellar spacing is the finest at 75 nm, with 0.02% Nb directly linking the superior elongation. The optimized composition of NB1 exhibits nearly double the %RA. Figure 2 illustrates the significant refinement of the pearlite.

The NB1 composition exhibits the finest interlamellar spacing at 75 nm.

The master rods were then drawn into the final prestressed wire rod product. Figure 4 relates the reduction of area to the strain ratio of the initial diameter to the final product diameter. The optimum strain ratio for the industrial wire drawing operation is between 1.50 and 1.80. The consistent 55% reduction of area ( $\mu$ -Nb with the 0.02% Nb eutectoid chemistry) over this strain ratio range is excellent (i.e., flat) and results in increased productivity at the wire rod mill.

The evolution of the reduction of area with the strain is highest for the Nb-containing steels. This result indicates the improvement in ductility due to the Nb addition.

**Industrial Trials** — Based on the laboratory results, an industrial heat was produced at a BOF operation. The Nb heat was continuously cast into billets with no problems, and the billet quality was excellent. Nineteen billets were hot rolled into 7.5-mm wire rods. The wire rods were shipped to two plants to manufacture strands for PSC applications. The mechanical properties of the wire rods were obtained from the beginning and end of each coil to check mechanical property consistency. The mean values of the ultimate tensile strength and the %RA are listed in Table 5.

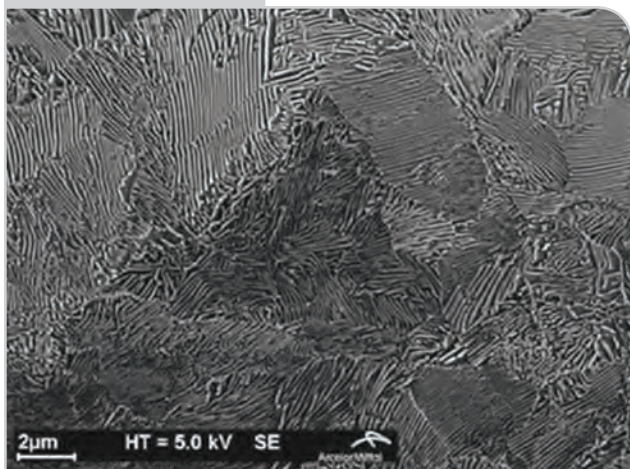
The quality of the 7.5-mm wire rod was evaluated. No axial segregation, surface damages or decarburization were observed. The 7.5-mm wire rod exhibited a homogeneous pearlitic microstructure even at the core (Figure 5). The entire heat of coils was processed successfully without any rolling process modifications. The required tensile strength in the final product of 2,160 N/mm<sup>2</sup> was achieved. The rolling process formed 2.4-mm drawn wires from the 7.5-mm wire rods. However, at one plant, an extra drawing pass was applied, which led to even higher tensile strength without any surface quality, cracking or forming issues.

Figure 5 illustrates the SEM micrograph of homogenous pearlitic microstructure even at the core of the 7.5-mm wire rod.

The curve in Figure 6 reflects the work-hardening behavior of the wires while being reduced by cold drawing at the two plants. As discussed earlier, this transformation corresponds to a strain in the region of approximately 1.5–1.8.

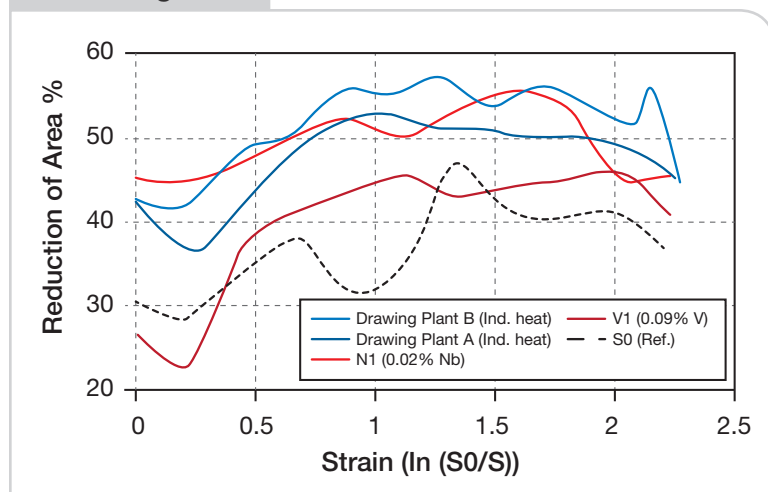


Figure 5



Homogeneous pearlitic eutectoid steel microstructure at 0.018% Nb in the core.

Figure 6



Reduction of area versus strain.

As a result of the higher Cr content, the work-hardening curves established from the plant-drawn rods are shifted to the upper part of the graph compared to the NB1 curve. The drawing plant B curve coincides with the laboratory-produced NB1 curve. The difference between the curves of plants B and A is due to the one extra 20% reduction pass. A comparison of the %RA improvement with Nb versus V shows a 30% improvement for plant A and a 20% improvement for plant B. Both plants experienced a 10% improvement in productivity due to the higher %RA.

## Discussion

This research has investigated the positive contribution of Nb at an optimized concentration (MicroNiobium

alloy approach) in high-carbon eutectoid steel for prestressed concrete wire rod. An improvement of the rheology has been confirmed on the cold drawn wires. The strength properties remain almost constant as the ductility increases.

The Nb micro-addition has a significant refinement effect on the microstructure and reduction of the interlamellar spacing. Through the refinement, an improvement in ductility (%RA) is experienced. Prior research has shown that the cementite thickness, which is directly connected to  $\lambda$ , is the most dominant microstructural factor affecting ductility.<sup>5</sup> During the cold drawing process of high-strength pearlitic wires, pearlite with smaller interlamellar spacing will realign faster to the drawing direction than coarse pearlite.<sup>6</sup> This phenomenon is independent of the transformation temperature and carbon content. This relationship

between %RA and  $\lambda$  for 0.52–0.92% C steels, where the MicroNiobium alloy approach is applied, is shown in Figure 7.

Figure 7 shows a maximum %RA for  $\lambda$  values in the range of 0.06–0.08  $\mu\text{m}$ . The  $\lambda$  values for the Nb steels is within this range, while the base steel (S0) and the V-bearing steels have  $\lambda$  values correlating to the downward slope of the curve at approximately 0.1  $\mu\text{m}$ .

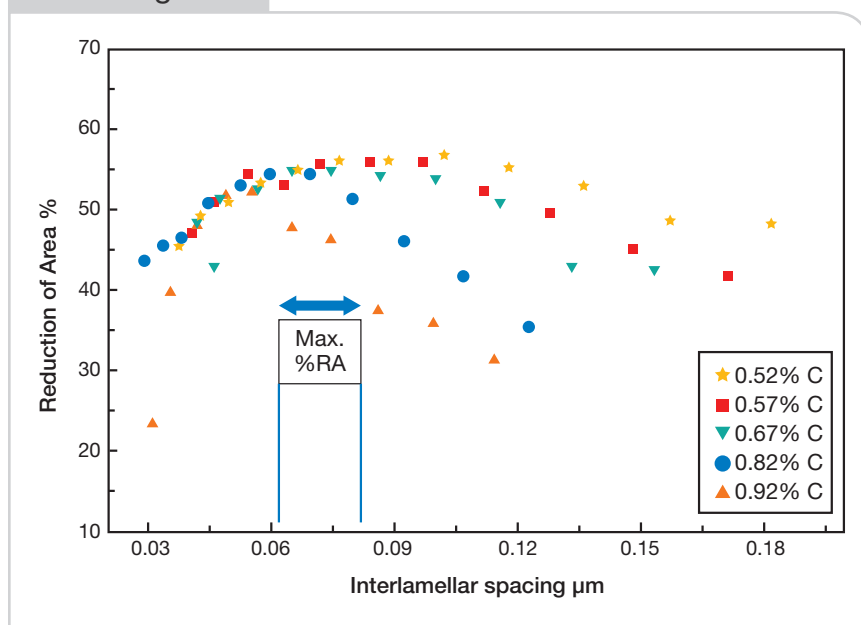
The refinement of the interlamellar spacing should improve the torsionability. The delamination occurring during torsion is initiated by the formation of voids around the globular cementite particles formed during the wire drawing process.<sup>6</sup> Hence, the higher the interlamellar spacing, the thicker the cementite lamellae and the larger the size of the globular cementite particles. This condition results in the observation of more frequent and larger voids. Thus, delamination will

occur earlier when initial interlamellar spacing is higher.

## Reheat Furnace Process Metallurgy and Abnormal Grain Growth

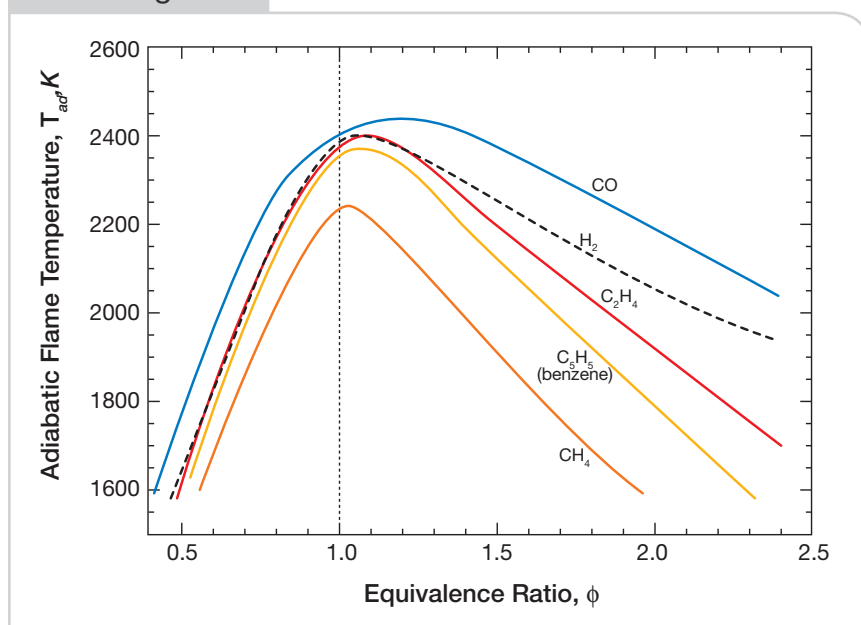
— The mechanism of abnormal grain growth is well established and documented.<sup>7</sup> However, the relationship between reheat furnace temperature and solubility of the microalloying elements at different carbon contents in actual industrial operations is difficult to correlate with laboratory studies and generated data. The quality and efficiency of the reheating process have a profound effect on the austenite grain size and uniformity of grain size along the entire length of the billet and the final product grain size.<sup>8</sup> This step in the steelmaking process often receives low priority in the evaluation of product quality and mechanical property performance. The homogeneity

Figure 7



% reduction of area vs. interlamellar spacing for cold drawn pearlitic steel (0.52–0.92% C).<sup>6</sup>

Figure 8



Air-to-gas equivalence ratio versus adiabatic flame temperature.<sup>8</sup>

the optimal adiabatic flame temperature performance. Effectively, variable adiabatic flame temperature means variations in the heat input to the steel and the austenite grain size. For example, in the case of a furnace firing with natural gas ( $\text{CH}_4$ ), the adiabatic flame temperature is shown as a function of the air-to-gas ratio in Figure 8.

As the air-to-gas equivalence ratio ( $\phi$ ) increases above 1.10, the adiabatic flame temperature decreases. As a consequence of the oxidizing furnace atmosphere, the iron oxide scale thickness also increases. The thicker scale acts as an insulating layer on the slab surface, thereby reducing the heat conduction efficiency. This variation in the heating process will significantly affect the resultant thermal homogeneity and gradient from the surface of the slab to the center of the billet, as well as the austenitic grain size and distribution.<sup>9</sup>

Therefore, discontinuous austenitic grain growth is directly influenced by such thermal variation conditions within the furnace caused by variable air-to-gas ratios. The effect of temperature and heating time on the prior austenite grain size is illustrated in Figure 9.<sup>10</sup> The connection between the process metallurgy and the physical metallurgy is made.

The relationship between the air-to-gas ratio, adiabatic flame temperature and the resultant austenite grain size may be correlated with the integration of Figures 8 and 9. The furnace operational process metallurgy can be converted to the reheating

and efficiency of heating are highly influenced by the air-to-gas ratio of the furnace burner combustion condition. The optimum air-to-gas ratio of 1.10 yields the highest adiabatic flame temperature.<sup>9</sup> However, often in actual operations, cracked burner orifice plates, poor burner tuning and inefficient combustion fan performance contribute to variations in the air-to-gas ratio. These situations have a huge influence on

temperature of the slab and then into the estimated austenite grain size. For example, if one section of the billet is at  $1,200^\circ\text{C}$  and the adjacent section is  $1,225^\circ\text{C}$  due to an air-to-gas variation of 0.05, then it follows that the austenite grain size would be approximately  $325\text{ }\mu\text{m}$  for the  $1,250^\circ\text{C}$  section versus the adjacent section at  $280\text{ }\mu\text{m}$  grain size for the  $1,225^\circ\text{C}$  region. Such differences in prior austenite grain size due to such

thermal variations in combustion lead to a variable ferrite grain size in the final hot rolled product and hence variable mechanical properties.

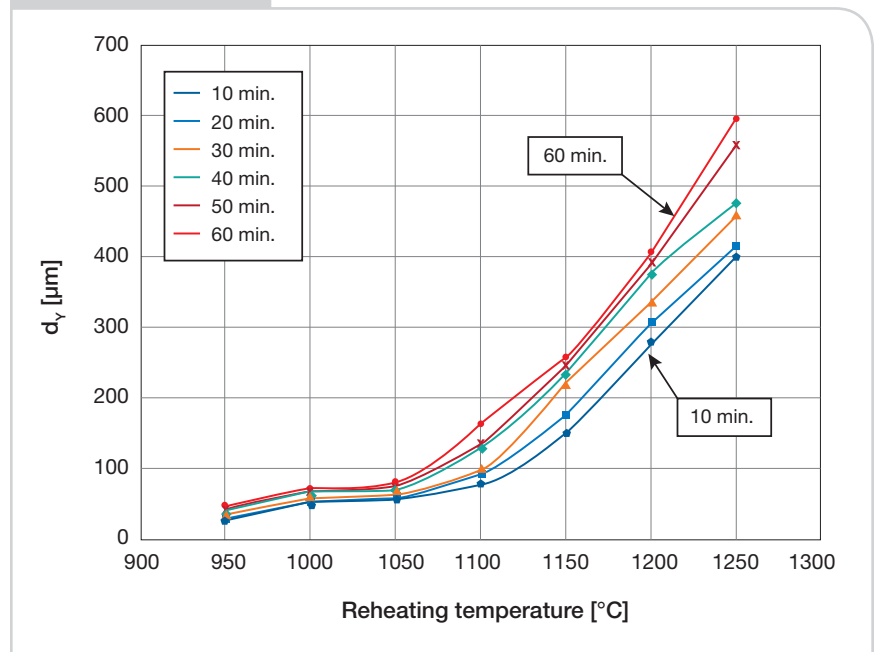
## Conclusions

The application of the MicroNiobium alloy approach in carbon steel long product and plate steels enhances both the metallurgical properties and processability and reduces the operational cost per metric ton. This study validates the application of 0.02% Nb in eutectoid steels with superior properties based on both laboratory and industrial trials. The process and product metallurgical improvements relate to the Nb-pinning effect of the austenite grain boundaries and the refinement effect in pearlitic eutectoid steel for pre-stressed concrete wire rod. With the temperature variations observed during the reheating process of the billets in an industrial operation, the metallurgical mechanism of the MicroNiobium alloy approach is also related to the retardation of austenite grain coarsening during reheat furnace soaking of the billet, slabs or shapes before rolling. Hence, a finer prior austenite grain size translates into finer interlamellar spacing in the pearlitic microstructure. Although the Nb solubility is limited in high-carbon steels, a very low 0.02% Nb suffices to produce significantly higher %RA compared to the standard PSC wire rod or V-bearing PSC wire rod, as illustrated in Table 4.

The high-strength properties were preserved in the Nb-bearing PSC along with excellent ductility in both the laboratory-generated heats and the industrial heats. Improved productivity (metric tons per hour) was evident during the cold drawing process at both plants. This value-added improvement offers the end user the opportunity to reduce operational costs when processing Nb-bearing PSC compared to the standard and V-bearing PSC.

The castability of the Nb-bearing PSC billets was excellent, and the billet surface quality exceeded the quality performance of the standard and V-bearing PSC billets, as illustrated in Table 3.

Figure 9



Austenite grain size versus reheating temperature.

## References

1. J.D. Embury and R.M. Fisher, "The Structure and Properties of Drawn Pearlite," *Acta Metallurgica*, Vol. 14, 1966, pp. 147–159.
2. D.A. Porter and K.E. Easterling, "Dynamic Studies of the Tensile Deformation and Fracture of Pearlite," *Acta Metallurgica*, Vol. 26, 1978, pp. 1405–1422.
3. W.J. Nam and C.M. Bae, "Void Initiation and Microstructural Changes During Wire Drawing of Pearlitic Steels," *Materials Science and Engineering*, Vol. 203, 1995, pp. 278–285.
4. Y.J. Park and I.M. Bernstein, "The Process of Crack Initiation and Effective Grain Size for Cleavage Fracture in Pearlitic Eutectoid Steels," *Metallurgical Transactions A*, Vol. 10A, 1979, pp. 1653–1664.
5. W.J. Nam, C.M. Bae, S.J. Oh and S.J. Kwon, "Effect of Interlamellar Spacing on Cementite Dissolution During Wire Drawing of Pearlitic Steel Wires," *Scripta Materialia*, Vol. 42, No. 5, 2000, pp. 457–463.
6. W.J. Nam, H.R. Song and C.M. Bae, "Effect of Microstructural Features on Ductility of Drawn Pearlitic Carbon Steels," *ISIJ International*, Vol. 45, No. 8, 2005, pp. 1205–1210.
7. P. Cotterill and P.R. Mould, *Recrystallization and Grain Growth in Metals*, Surrey University Press, New York, 1976, pp. 266–275.
8. *North American Combustion Handbook*, 2nd edition, 1978, pp. 1–14.
9. S. Jansto, "MicroNiobium Alloy Approach in Medium- and High-Carbon Bar, Plate and Sheet Products," *AMPT2012 Conference*, Wollongang, Australia, 23–26 September 2012.
10. L. Nemethova, *Acta Metallurgica Slovaca*, Vol. 15, No. 3, 2009, pp. 173–179. ♦



To nominate this paper for the AIST Hunt-Kelly Outstanding Paper Award, visit [AIST.org/huntkelly](http://AIST.org/huntkelly).

This paper was presented at AISTech 2014 — The Iron & Steel Technology Conference and Exposition, Indianapolis, Ind., and published in the Conference Proceedings.